Computing photonic band structures by Dirichlet-to-Neumann maps: the triangular lattice

Jianhua Yuan

Department of Mathematics, Beijing University of Posts and Telecommunications

Beijing, China

Ya Yan Lu *

Department of Mathematics, City University of Hong Kong

Kowloon, Hong Kong

Abstract

An efficient semi-analytic method is developed for computing the band structures of two-dimensional photonic crystals which are triangular lattices of circular cylinders. The problem is formulated as an eigenvalue problem for a given frequency using the Dirichlet-to-Neumann (DtN) map of a hexagon unit cell. This is a linear eigenvalue problem even if the material is dispersive, where the eigenvalue depends on the Bloch wave vector. The DtN map is constructed from a cylindrical wave expansion, without using sophisticated lattice sums techniques. The eigenvalue problem can be efficiently solved by standard linear algebra programs, since it involves only matrices of relatively small size.

1 Introduction

Photonic crystals [1] are artificial periodic structures with a period on the order of the optical wavelength. An important property of a photonic crystal is the existence of photonic bandgaps. Light corresponding to a frequency in a bandgap cannot propagate inside the structure in any direction. Photonic crystals are being extensively studied due to their unusual ability to manipulate light and their many potential applications.

Efficient numerical methods are essential to the design and optimization of photonic crystals and related devices. Given a photonic crystal, a fundamental problem is to compute its band structures. In the standard formulation [1], this is an eigenvalue problem

*Tel.: +852-27887436; fax: +852-27887446. *Email address*: mayylu@cityu.edu.hk (Y. Y. Lu).

of a differential operator defined on the unit cell (i.e. one period) of the structure, where ω^2 (ω is the angular frequency) is the eigenvalue and the components of the Bloch wave vector are given parameters. For a non-dispersive medium, this is a linear eigenvalue problem that can be discretized by various numerical methods including the plane-wave-expansion method [2, 3, 4, 5, 6], the finite element method [7, 8], the finite difference method [9, 10, 11], the cell method [12], the moving least squares method [13], the wavelet method [14], etc. For a dispersive medium, this formulation gives rise to a more difficult nonlinear eigenvalue problem. On the other hand, a nonlinear eigenvalue problem (even when the medium is non-dispersive) of a much smaller matrix can be obtained using a cylindrical/spherical wave expansion [15, 16, 17]. In this case, the eigenvalue is still ω^2 and it can only be determined one by one from the condition that a matrix becomes singular.

A different approach to band structure computation is to assume that the frequency ω is a given parameter and the eigenvalue is related to the Bloch wave vector. Linear eigenvalue problems can be formulated even for dispersive media based on the transfer matrix [18, 19] or the scattering matrices [20], although the transfer matrix approach suffers numerical instability. Different numerical methods can be used to compute the scattering matrices. If a cylindrical wave expansion is used, sophisticated lattice sums techniques are needed. Time domain methods [21, 22, 23] have also been developed for bandgap calculations, but they appear to be less efficient.

In a recent paper [24], we developed a Dirichlet-to-Neumann (DtN) map method for computing band structures of two-dimensional (2D) photonic crystals composed of a square lattice of parallel cylinders. Like the formulations based on the transfer and scattering matrices, we obtain a linear eigenvalue problem even when the medium is dispersive. Our method relies on the DtN operator that maps the wave field on the boundary of the unit cell to its normal derivative. For photonic crystals with unit cells containing circular cylinders, the DtN map can be approximated by a small matrix using cylindrical wave expansions. Unlike other techniques based on cylindrical wave expansions, the DtN map can be easily constructed without using sophisticated lattice sums techniques.

In this paper, we extend the DtN map method to photonic crystals composed of a triangular lattice of parallel cylinders. In the standard formulation [1] using ω^2 as the eigenvalue, there is almost no difference between a square lattice and a triangulate lattice. This is not the case for the DtN map method. For a square lattice, we obtained linear eigenvalue problems of $(4N) \times (4N)$ matrices [24], where N is the number of collocation points on each edge of the square unit cell. For the triangular lattice considered in this paper, we use a hexagon unit cell and obtain linear eigenvalue problems of $(12N) \times (12N)$ matrices, where N is the number of collocation points on each edge of the hexagon. The

eigenvalue problems are formulated on edges of the irreducible Brillouin zone at a fixed frequency. However, we have to replace one edge of the standard triangular irreducible Brillouin zone in order to avoid a further increase of the matrix size. Fortunately, a small N is sufficient to obtain accurate solutions. Numerical examples involving both dispersive and non-dispersive media are used to illustrate the accuracy and efficiency of our method.

2 Dirichlet-to-Neumann map of a hexagon unit cell

We consider a two-dimensional photonic crystal composed of circular cylinders (parallel to the z-axis) with a dielectric constant ϵ_1, embedded in a background medium with a dielectric constant ϵ_2. On the xy-plane, the cylinders form a triangular lattice with translation vectors $\mathbf{a}_1 = (L, 0)$ and $\mathbf{a}_2 = (L/2, \sqrt{3}L/2)$, where L is the lattice constant. Therefore, the relative dielectric function satisfies

$$\epsilon(\mathbf{x}) = \epsilon(\mathbf{x} + l_1\mathbf{a}_1 + l_2\mathbf{a}_2), \tag{1}$$

where $\mathbf{x} = (x, y)$, l_1 and l_2 are arbitrary integers. Let a be the radius of the circular cross section of the cylinders, we have

$$\epsilon(\mathbf{x}) = \begin{cases} \epsilon_1, & \text{if } |\mathbf{x} - l_1\mathbf{a}_1 - l_2\mathbf{a}_2| < a \text{ for integers } l_1 \text{ and } l_2, \\ \epsilon_2, & \text{otherwise.} \end{cases}$$

For two-dimensional problems, the governing equations are

$$\frac{\partial^2 u}{\partial x^2} + \frac{\partial^2 u}{\partial y^2} + k_0^2 \epsilon\, u = 0 \tag{2}$$

for the E polarization and

$$\frac{\partial}{\partial x}\left(\frac{1}{\epsilon}\frac{\partial u}{\partial x}\right) + \frac{\partial}{\partial y}\left(\frac{1}{\epsilon}\frac{\partial u}{\partial y}\right) + k_0^2 u = 0 \tag{3}$$

for the H polarization, where $k_0 = \omega/c$ is the free space wavenumber, c is the speed of light in vacuum and u is the z-component of the electric or magnetic fields, respectively. Our method relies on the DtN map of a unit cell of the photonic crystal. For the triangular lattice specified above, we choose the hexagon unit cell $ABCDEF$ as shown in Fig. 1. Let Γ be the boundary of the hexagon unit cell, the DtN operator Λ satisfies

$$\Lambda\, u|_\Gamma = \left.\frac{\partial u}{\partial \nu}\right|_\Gamma, \tag{4}$$

where ν is a unit vector defined on the boundary Γ.

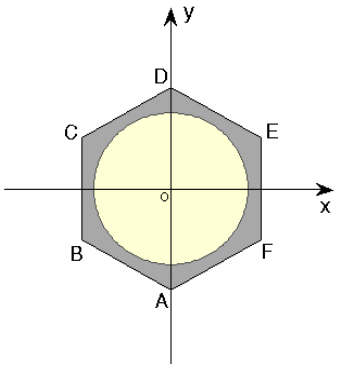

Figure 1: The hexagon unit cell for a triangular lattice.

To construct a matrix approximation to the operator Λ, we write down the general solution of the Helmholtz equations (2) and (3) using the polar coordinate system (r, θ). We have

$$u(\mathbf{x}) = \sum_{m=-\infty}^{\infty} C_m \Phi_m(r,\theta), \quad \Phi_m(r,\theta) = \phi_m(r) e^{im\theta}, \tag{5}$$

where $\phi_m(r)$ is related to the Bessel functions J_m and Y_m as

$$\phi_m(r) = \begin{cases} A_m J_m(k_0 n_1 r), & r < a; \\ B_m J_m(k_0 n_2 r) + Y_m(k_0 n_2 r), & r > a. \end{cases}$$

Here, n_1 and n_2 are the refractive indices satisfying $n_j = \sqrt{\epsilon_j}$ for $j = 1, 2$. The coefficients A_m and B_m can be solved from the interface conditions at $r = a$ for the two polarizations, respectively [24]. If we choose N points on each edge of the hexagon and truncate the general solution (5) to $6N$ terms (for $-3N \le m < 3N$), then the u values at the $6N$ points on the boundary of the hexagon can be related to the coefficients $\{C_m\}$ by

$$u(\mathbf{x}_j) = \sum_{m=-3N}^{3N-1} C_m \Phi_m(r_j, \theta_j),$$

where $\mathbf{x}_j$ for $1 \le j \le 6N$ are the points on the boundary of the hexagon, (r_j, θ_j) are the polar coordinates of $\mathbf{x}_j$. This gives rise to a $(6N) \times (6N)$ matrix Λ_1 that maps the coefficients $\{C_m\}$ to the u values on the boundary. The entries of Λ_1 are $\Phi_m(r_j, \theta_j)$ for $1 \le j \le 6N$ and $-3N \le m < 3N$. Meanwhile, the derivatives of u can be evaluated analytically from its general solution (5). Let $\nu(\mathbf{x}_j)$ be a unit normal vector at the point $\mathbf{x}_j$ on the boundary, we have

$$\left.\frac{\partial u}{\partial \nu}\right|_{\mathbf{x}=\mathbf{x}_j} = \sum_{m=-3N}^{3N-1} C_m \nu(\mathbf{x}_j) \cdot \nabla \Phi_m|_{\mathbf{x}=\mathbf{x}_j}.$$

This gives rise to a $(6N) \times (6N)$ matrix Λ_2 that maps the coefficients $\{C_m\}$ to the normal derivative of u on the boundary of the hexagon. The entries of Λ_2 are $\nu(\mathbf{x}_j) \cdot \nabla \Phi_m|_{\mathbf{x}=\mathbf{x}_j}$

for $1 \le j \le 6N$ and $-3N \le m < 3N$. Therefore, the matrix approximation of the DtN operator of the hexagon is given by

$$\Lambda = \Lambda_2 \Lambda_1^{-1}. \tag{6}$$

Clearly, $O(N^3)$ operations are required to compute Λ.

In the following, we choose N equally-spaced points on each edge of the hexagon. Since the length of an edge is $L/\sqrt{3}$, the distance between two nearby points on the same edge is $L/(\sqrt{3}N)$. The first and last points on each edge are chosen to have one half of that distance (i.e. $L/(2\sqrt{3}N)$) to the nearby vertices. Furthermore, the unit normal vectors on opposite edges of the hexagon are chosen to be the same. For the edges $\overrightarrow{AB}$, $\overrightarrow{BC}$ and $\overrightarrow{CD}$, $\nu(\mathbf{x})$ is the inward unit normal vector. For the other three edges, it is the outward unit normal vector.

3 Eigenvalue problems

To analyze band structures of a two-dimensional photonic crystal, we consider Bloch mode solutions of Eq. (2) or (3) given as

$$u(x, y) = e^{i(\alpha x + \beta y)} \Psi(x, y), \tag{7}$$

where (α, β) is a real Bloch wave vector and Ψ follows the same periodic condition (1) as the dielectric function. In the following, we formulate an eigenvalue problem for a given angular frequency ω, where the eigenvalue is related to α or β.

For the hexagon unit cell shown in Fig. 1, we denote u on the edges $\overrightarrow{AB}$, $\overrightarrow{BC}$, ..., $\overrightarrow{FA}$ by u_0, v_0, w_0, u_1, v_1, w_1, respectively. We also denote the corresponding normal derivative by $\partial_\nu u_0$, $\partial_\nu v_0$, etc. For the Bloch mode solution (7), the periodicity of the structure leads to

$$u_1 = \rho_\alpha \rho_\beta u_0, \qquad \partial_\nu u_1 = \rho_\alpha \rho_\beta \, \partial_\nu u_0, \tag{8}$$

$$v_1 = \rho_\alpha^2 v_0, \qquad \partial_\nu v_1 = \rho_\alpha^2 \, \partial_\nu v_0, \tag{9}$$

$$\rho_\beta w_1 = \rho_\alpha w_0, \qquad \rho_\beta \, \partial_\nu w_1 = \rho_\alpha \, \partial_\nu w_0, \tag{10}$$

where $\rho_\alpha = \exp(i\alpha L/2)$ and $\rho_\beta = \exp(i\sqrt{3}\beta L/2)$. In the discrete case, u_0, $\partial_\nu u_0$, ..., are column vectors of length N and the DtN map Λ is a $(6N) \times (6N)$ matrix. If Λ is partitioned as a 6×6 block matrix where each block is an $N \times N$ matrix, we can write

down Eq. (4) as

$$\begin{bmatrix} \Lambda_{11} & \Lambda_{12} & \Lambda_{13} & \Lambda_{14} & \Lambda_{15} & \Lambda_{16} \\ \Lambda_{21} & \Lambda_{22} & \Lambda_{23} & \Lambda_{24} & \Lambda_{25} & \Lambda_{26} \\ \Lambda_{31} & \Lambda_{32} & \Lambda_{33} & \Lambda_{34} & \Lambda_{35} & \Lambda_{36} \\ \Lambda_{41} & \Lambda_{42} & \Lambda_{43} & \Lambda_{44} & \Lambda_{45} & \Lambda_{46} \\ \Lambda_{51} & \Lambda_{52} & \Lambda_{53} & \Lambda_{54} & \Lambda_{55} & \Lambda_{56} \\ \Lambda_{61} & \Lambda_{62} & \Lambda_{63} & \Lambda_{64} & \Lambda_{65} & \Lambda_{66} \end{bmatrix} \begin{bmatrix} u_0 \\ v_0 \\ w_0 \\ u_1 \\ v_1 \\ w_1 \end{bmatrix} = \begin{bmatrix} \partial_\nu u_0 \\ \partial_\nu v_0 \\ \partial_\nu w_0 \\ \partial_\nu u_1 \\ \partial_\nu v_1 \\ \partial_\nu w_1 \end{bmatrix}. \tag{11}$$

Using the periodic conditions (8-10), we can eliminate u_1, v_1, w_1, $\partial_\nu u_0$,$\partial_\nu v_0$, $\partial_\nu w_0$, $\partial_\nu u_1$, $\partial_\nu v_1$ and $\partial_\nu w_1$ and obtain

$$\begin{bmatrix} \Lambda_{41} & \Lambda_{42} & \Lambda_{43} \\ \Lambda_{51} & \Lambda_{52} & \Lambda_{53} \\ \Lambda_{61} & \Lambda_{62} & \Lambda_{63} \end{bmatrix} \begin{bmatrix} u_0 \\ v_0 \\ w_0 \end{bmatrix} = \begin{bmatrix} M_{11} & M_{12} & M_{13} \\ M_{21} & M_{22} & M_{23} \\ M_{31} & M_{32} & M_{33} \end{bmatrix} \begin{bmatrix} u_0 \\ v_0 \\ w_0 \end{bmatrix}, \tag{12}$$

where M_{ij} are $N \times N$ matrices given by

$$\begin{aligned} M_{11} &= \rho_\alpha \rho_\beta (\Lambda_{11} - \Lambda_{44}) + \rho_\alpha^2 \rho_\beta^2 \Lambda_{14}, \\ M_{12} &= \rho_\alpha \rho_\beta \Lambda_{12} - \rho_\alpha^2 \Lambda_{45} + \rho_\alpha^3 \rho_\beta \Lambda_{15}, \\ M_{13} &= \rho_\alpha \rho_\beta \Lambda_{13} + \rho_\alpha^2 \Lambda_{16} - \frac{\rho_\alpha}{\rho_\beta} \Lambda_{46}, \\ M_{21} &= \rho_\alpha^2 \Lambda_{21} - \rho_\alpha \rho_\beta \Lambda_{54} + \rho_\alpha^3 \rho_\beta \Lambda_{24}, \\ M_{22} &= \rho_\alpha^2 (\Lambda_{22} - \Lambda_{55}) + \rho_\alpha^4 \Lambda_{25}, \\ M_{23} &= \rho_\alpha^2 \Lambda_{23} - \frac{\rho_\alpha}{\rho_\beta} \Lambda_{56} + \frac{\rho_\alpha^3}{\rho_\beta} \Lambda_{26}, \\ M_{31} &= \rho_\alpha^2 \Lambda_{34} + \frac{\rho_\alpha}{\rho_\beta} \Lambda_{31} - \rho_\alpha \rho_\beta \Lambda_{64}, \\ M_{32} &= \frac{\rho_\alpha}{\rho_\beta} \Lambda_{32} - \rho_\alpha^2 \Lambda_{65} + \frac{\rho_\alpha^3}{\rho_\beta} \Lambda_{35}, \\ M_{33} &= \frac{\rho_\alpha}{\rho_\beta} (\Lambda_{33} - \Lambda_{66}) + \frac{\rho_\alpha^2}{\rho_\beta^2} \Lambda_{36}. \end{aligned}$$

For the triangular lattice of circular cylinders, we only have to find Bloch mode solutions (7) for (α, β) in the irreducible Brillouin zone, which is the triangular region with corners at $\Gamma(\alpha = \beta = 0)$, $M(\alpha = 0, \beta = \frac{2\pi}{\sqrt{3}L})$ and $K(\alpha = \frac{2\pi}{3L}, \beta = \frac{2\pi}{\sqrt{3}L})$ shown in Fig. 2. As in most bandgap calculations, we compute the dispersion relations for (α, β) on the boundary of the triangle ΓMK. From Γ to M, we have $\rho_\alpha = 1$. Therefore, we can regard ρ_β as the eigenvalue. From M to K, we can formulate an eigenvalue problem for ρ_α since $\rho_\beta = -1$. From K to Γ, we have $\rho_\alpha^3 = \rho_\beta$ and the eigenvalue problem becomes somewhat more complicated. However, due to the rotational symmetry of photonic crystals, the dispersion relations on the edge $K\Gamma$ are equivalent to those on $K'\Gamma$ for

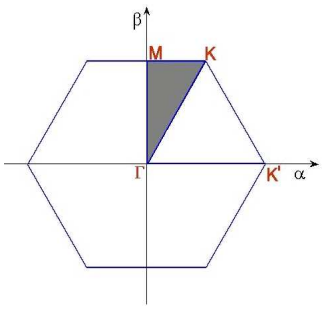

Figure 2: The Brillouin zone of a triangular lattice of dielectric columns.

$K'(\alpha = \frac{4\pi}{3L}, \beta = 0)$ shown in Fig. 2. From K' to Γ, we have $\rho_\beta = 1$, therefore, ρ_α can be regarded as the eigenvalue. In conclusion, Eq. (12) can be written as the following nonlinear eigenvalue problem:

$$\left[\lambda^4\mathbb{M}_4 + \lambda^3\mathbb{M}_3 + \lambda^2\mathbb{M}_2 + \lambda\mathbb{M}_1 + \mathbb{M}_0\right]\mathbf{U} = 0. \tag{13}$$

where $\mathbf{U} = (u_0, v_0, w_0)^T$. The eigenvalue λ and the matrices $\mathbb{M}_0$, ..., $\mathbb{M}_4$ are defined on each edge as follows:

1. From Γ to M, $\lambda = \rho_\beta$ for $0 < \beta \leq \frac{2\pi}{\sqrt{3}L}$ and

$$\mathbb{M}_4 = \begin{bmatrix} -\Lambda_{14} & 0 & 0 \\ 0 & 0 & 0 \\ 0 & 0 & 0 \end{bmatrix}, \quad \mathbb{M}_3 = \begin{bmatrix} \Lambda_{44} - \Lambda_{11} & -\Lambda_{12} - \Lambda_{15} & -\Lambda_{13} \\ \Lambda_{54} - \Lambda_{24} & 0 & 0 \\ \Lambda_{64} & 0 & 0 \end{bmatrix},$$

$$\mathbb{M}_2 = \begin{bmatrix} \Lambda_{41} & \Lambda_{42} + \Lambda_{45} & \Lambda_{43} - \Lambda_{16} \\ \Lambda_{51} - \Lambda_{21} & \Lambda_{55} - \Lambda_{22} + \Lambda_{52} - \Lambda_{25} & \Lambda_{53} - \Lambda_{23} \\ \Lambda_{61} - \Lambda_{34} & \Lambda_{65} + \Lambda_{62} & \Lambda_{63} \end{bmatrix},$$

$$\mathbb{M}_1 = \begin{bmatrix} 0 & 0 & \Lambda_{46} \\ 0 & 0 & \Lambda_{56} - \Lambda_{26} \\ -\Lambda_{31} & -\Lambda_{32} - \Lambda_{35} & \Lambda_{66} - \Lambda_{33} \end{bmatrix}, \quad \mathbb{M}_0 = \begin{bmatrix} 0 & 0 & 0 \\ 0 & 0 & 0 \\ 0 & 0 & -\Lambda_{36} \end{bmatrix}.$$

2. From M to K, $\lambda = \rho_\alpha$ for $0 < \alpha \leq \frac{2\pi}{3L}$ and

$$\mathbb{M}_4 = \begin{bmatrix} 0 & 0 & 0 \\ 0 & -\Lambda_{25} & 0 \\ 0 & 0 & 0 \end{bmatrix}, \quad \mathbb{M}_3 = \begin{bmatrix} 0 & \Lambda_{15} & 0 \\ \Lambda_{24} & 0 & \Lambda_{26} \\ 0 & \Lambda_{35} & 0 \end{bmatrix},$$

$$\mathbb{M}_2 = \begin{bmatrix} -\Lambda_{14} & \Lambda_{45} & -\Lambda_{16} \\ -\Lambda_{21} & \Lambda_{55} - \Lambda_{22} & -\Lambda_{23} \\ -\Lambda_{34} & \Lambda_{65} & -\Lambda_{36} \end{bmatrix}, \quad \mathbb{M}_1 = \begin{bmatrix} \Lambda_{11} - \Lambda_{44} & \Lambda_{12} & \Lambda_{13} - \Lambda_{46} \\ -\Lambda_{54} & 0 & -\Lambda_{56} \\ \Lambda_{31} - \Lambda_{64} & \Lambda_{32} & \Lambda_{33} - \Lambda_{66} \end{bmatrix},$$

$$\mathbb{M}_0 = \begin{bmatrix} \Lambda_{41} & \Lambda_{42} & \Lambda_{43} \\ \Lambda_{51} & \Lambda_{52} & \Lambda_{53} \\ \Lambda_{61} & \Lambda_{62} & \Lambda_{63} \end{bmatrix}.$$

3. From K' to Γ, $\lambda = \rho_\alpha$ for $0 < \alpha \leq \frac{4\pi}{3L}$, the matrices $\mathbb{M}_0$, $\mathbb{M}_2$ and $\mathbb{M}_4$ are identical to those in case 2 above, $\mathbb{M}_1$ and $\mathbb{M}_3$ have an opposite sign as those in case 2.

Although the polynomial eigenvalue problem (13) is nonlinear, it can be easily transformed to the following linear eigenvalue problem

$$\lambda \begin{bmatrix} \mathbb{M}_4 & & & \\ & I & & \\ & & I & \\ & & & I \end{bmatrix} \mathbf{V} + \begin{bmatrix} \mathbb{M}_3 & \mathbb{M}_2 & \mathbb{M}_1 & \mathbb{M}_0 \\ -I & 0 & 0 & 0 \\ 0 & -I & 0 & 0 \\ 0 & 0 & -I & 0 \end{bmatrix} \mathbf{V} = 0, \tag{14}$$

where I is the identify matrix and $\mathbf{V} = [\lambda^3 \mathbf{U}^T, \lambda^2 \mathbf{U}^T, \lambda \mathbf{U}^T, \mathbf{U}^T]^T$. With N points on each edge of the hexagon unit cell, the matrices $\mathbb{M}_j$ for $0 \leq j \leq 4$ are $(3N) \times (3N)$ matrices. Therefore, (14) is a linear eigenvalue problem of $(12N) \times (12N)$ matrices. Since N is typically very small (e.g. $N \leq 10$), the matrices in (14) are still much smaller than those obtained by the plane wave expansion method or the finite element method.

4 Numerical examples

In this section, we apply the DtN method to a number of examples including both dispersive and non-dispersive media. As usual, we show dispersion curves for Bloch wave vector (α, β) along the boundary of the irreducible Brillouin zone. Our method is especially suitable for computing the bandgaps directly. In this connection, we calculate "gap maps" that display the dependence of bandgaps on the ratio between the radius a of the cylinders and the lattice constant L. All our results are obtained with $N = 9$, where N is the number of collocation points used on each edge of the hexagon unit cell. This implies that the DtN map of the unit cell is constructed from a cylindrical wave expansion of 54 terms and the linear eigenvalue problem involves 108×108 matrices.

We first consider an example studied in [1, 25]. The photonic crystal consists of a triangular lattice of air columns ($\epsilon_1 = 1.0$) in a dielectric medium ($\epsilon_2 = 13$). The radius of the circular air columns satisfies $a/L = 0.48$. The dispersion curves for both polarizations are plotted in Fig. 3. The vertical axis is the normalized frequency $\omega L/(2\pi c)$. The horizontal axis represents edges of the irreducible Brillouin zone. A complete bandgap for both polarizations can be observed in Fig. 3. Our calculations confirm the recent finite difference results [25] obtained from the eigenvalue problem of a sparse 65536×65536 matrix (as a discretization of a 256×256 grid).

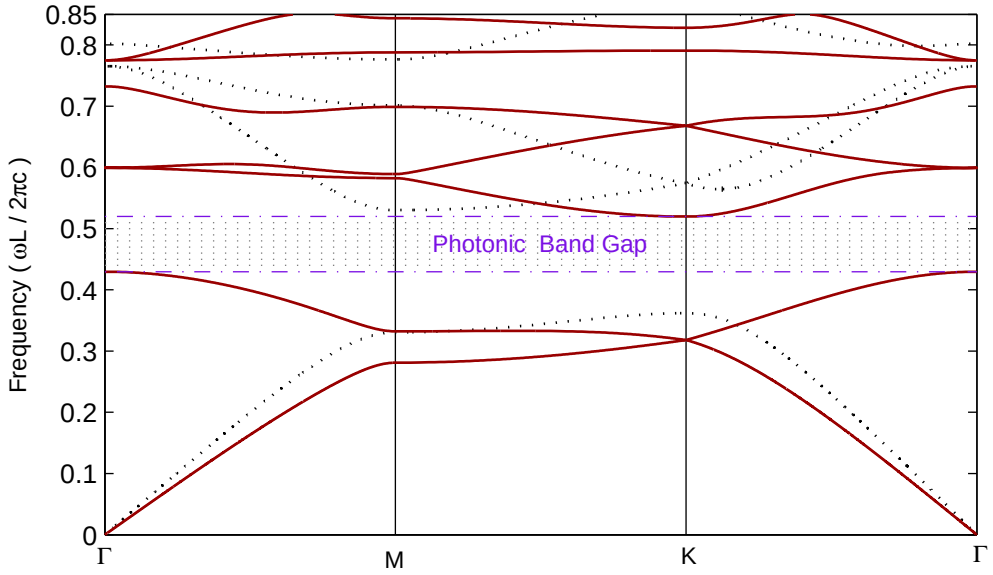

Figure 3: Band structure for a triangular lattice of air columns (radius $a = 0.48L$) in a dielectric medium ($\epsilon_2 = 13$). The solid and dashed lines represent the E and H polarizations, respectively.

The second example is concerned with a triangular lattice of dielectric cylinders in vacuum. The dielectric constant and the radius of the cylinders are $\epsilon_1 = 5$ and $a = 0.2158L$, respectively. The structure has been analyzed earlier by the plane wave expansion method [26] and the finite element method [8]. In Fig. 4, we show the dispersion curves obtained from our method. We can see that there are bandgaps for the E and H polarizations separately, but there is no complete bandgap for $\omega L/2\pi c < 1.2$. Our results are nearly identical to those in [8] and [26].

Our method can be used to analyze photonic crystals composed of dispersive materials without any difficulty. In particular, the eigenvalue problem (14) remains linear when the dielectric function ϵ depends on ω. To validate our method for the dispersive case, we consider two examples previously studied by Kuzmiak *et al.* in [27] and [28]. The structure considered in [27] consists of a triangular lattice of metallic cylinders in vacuum. The relative dielectric function of the metallic cylinders is assumed to satisfy the simple Drude model:

$$\epsilon_1(\omega) = 1 - \frac{\omega_p^2}{\omega^2}, \tag{15}$$

where ω_p is the plasma frequency of the conduction electrons. In the following, we assume that $\omega_p = 2\pi c/L$ and choose the radius of the cylinders $a = 0.3713L$, which corresponds to a filling fraction (the ratio between the areas of the cross section of a cylinder and a unit cell) of $f \approx 0.5$. The dispersion curves computed by our method are plotted in

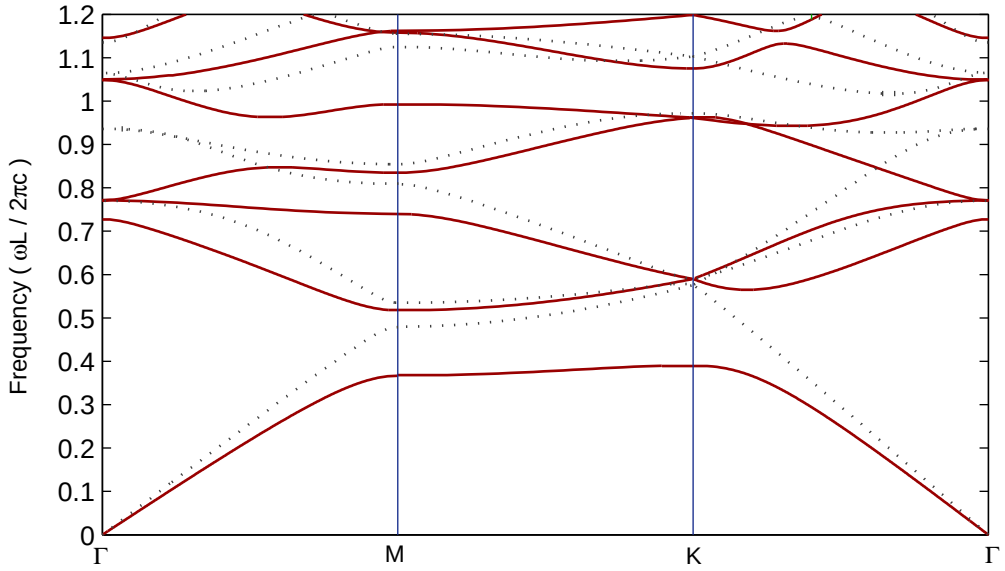

Figure 4: Band structure for a triangular lattice of dielectric cylinders ($\epsilon_1 = 5.0$, radius $a = 0.2158L$) in vacuum. The solid and dashed lines represent the E and H polarizations, respectively.

Fig. 5. We also consider an example studied in [28]. The structure consists of a triangular lattice of cylinders in vacuum, where the cylinders are made from a cubic, polar, diatomic crystal. The relative dielectric function of the cylinders is assumed to satisfy

$$\epsilon_1(\omega) = \epsilon_\infty \frac{\omega_L^2 - \omega^2}{\omega_T^2 - \omega^2},$$

where ϵ_∞ is the optical frequency dielectric constant, ω_L and ω_T are the frequencies of the longitudinal optical and transverse optical vibration modes of infinite wavelength, respectively. As in [28], we choose

$$\epsilon_\infty = 10.9, \quad \omega_T = 2\pi c/L, \quad \omega_L = 1.07759\,\omega_T$$

and $a = 0.2878L$ which corresponds to a filling fraction of $f \approx 0.3$. We calculate the band structures for both polarizations by our DtN method. The dispersion curves are plotted in Fig. 6. The results in [27] and [28] are obtained by the plane wave expansion method which gives rise to a nonlinear eigenvalue problem for a dispersive material.

Our DtN method is particularly suitable for computing bandgaps without first calculating the detailed dispersion curves. For the eigenvalue problem (14), the eigenvalue λ is either $\exp(i\alpha L/2)$ or $\exp(i\sqrt{3}\beta L/2)$, where (α, β) is the Bloch wave vector. On a dispersion curve, there is a Bloch mode solution (7) with real α and β which gives rise to

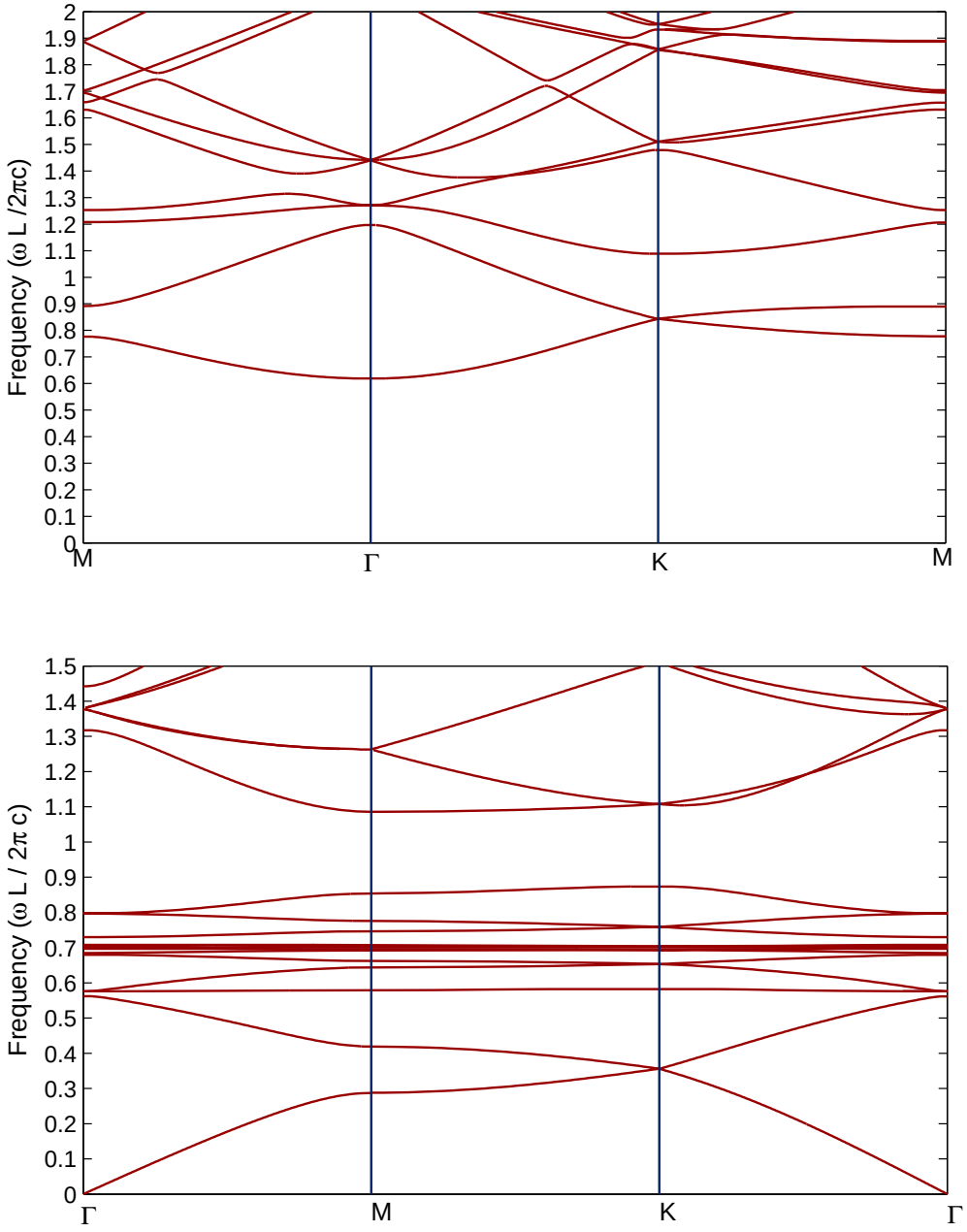

Figure 5: Band structures of a triangular lattice of metallic cylinders (radius $a = 0.3713L$) in vacuum for the E polarization (top) and H polarization (bottom).

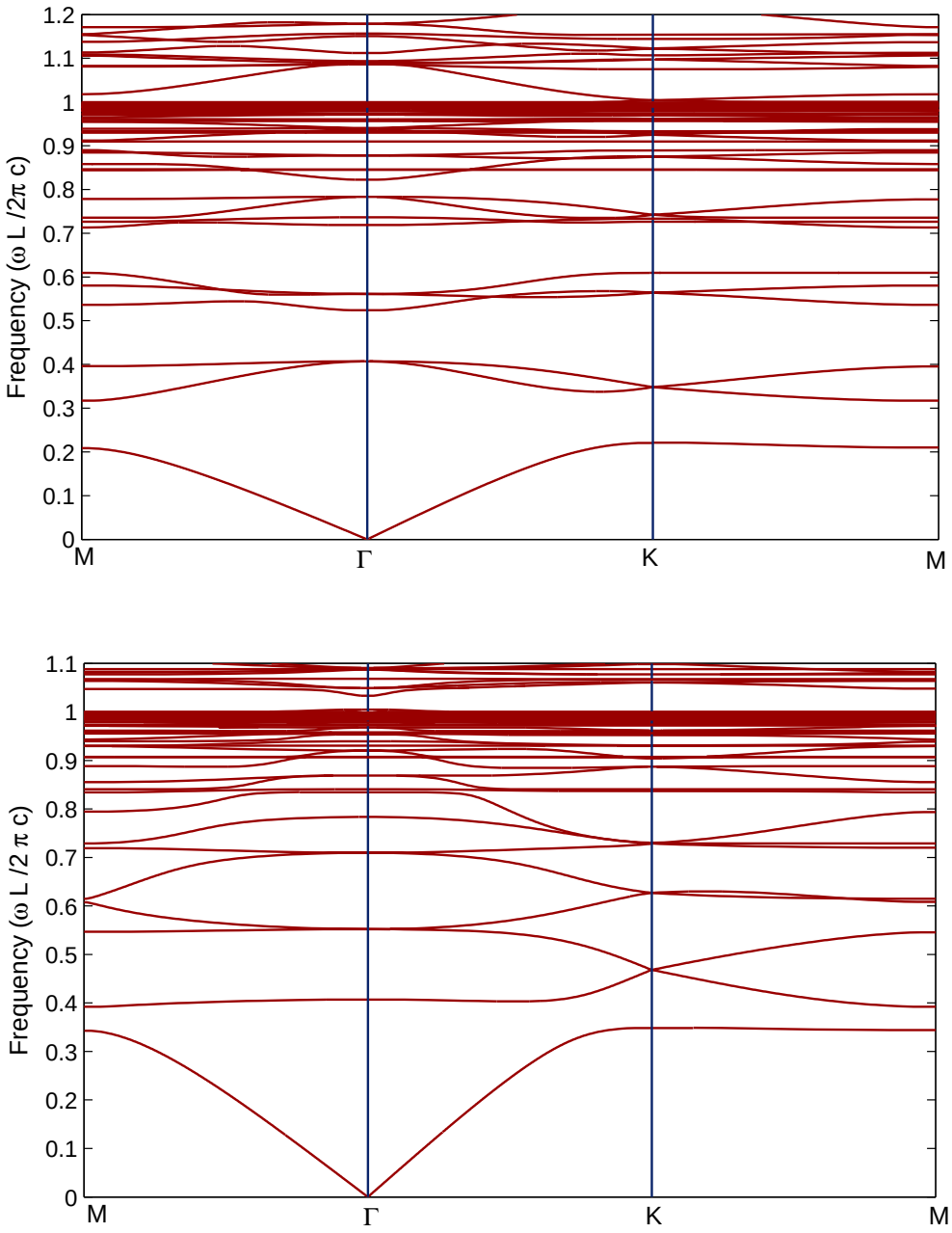

Figure 6: Band structures of a triangular lattice of cylinders (cubic, polar, diatomic crystal, with radius $a = 0.2878L$) in vacuum for the E polarization (top) and H polarization (bottom).

an eigenvalue satisfying $|\lambda| = 1$. In a bandgap, no eigenvalues can satisfy $|\lambda| = 1$, since there are only Bloch mode solutions with complex α or β. Furthermore, the eigenvalues appear in pairs as (λ_1, λ_2) satisfying $\lambda_1\lambda_2 = 1$. Therefore, we can define a function of the frequency ω as

$$F(\omega) = \min\{1 - |\lambda|, \quad \lambda \text{ is an eigenvalue of (14) satisfying } |\lambda| \leq 1\},$$

such that $F(\omega) > 0$ if and only if ω is inside a bandgap. The bandgaps can be found by searching the intervals where F is positive. This can be done by a simple bisection method. We have used this method to compute the "gap maps" that reveal the dependence of bandgaps on the radius of the cylinders. For a triangular lattice of air columns in the dielectric medium with a dielectric constant $\epsilon_2 = 11.4$, we obtain the gap map in Fig. 7. The bandgaps for the E and H polarizations only are marked in red and blue,

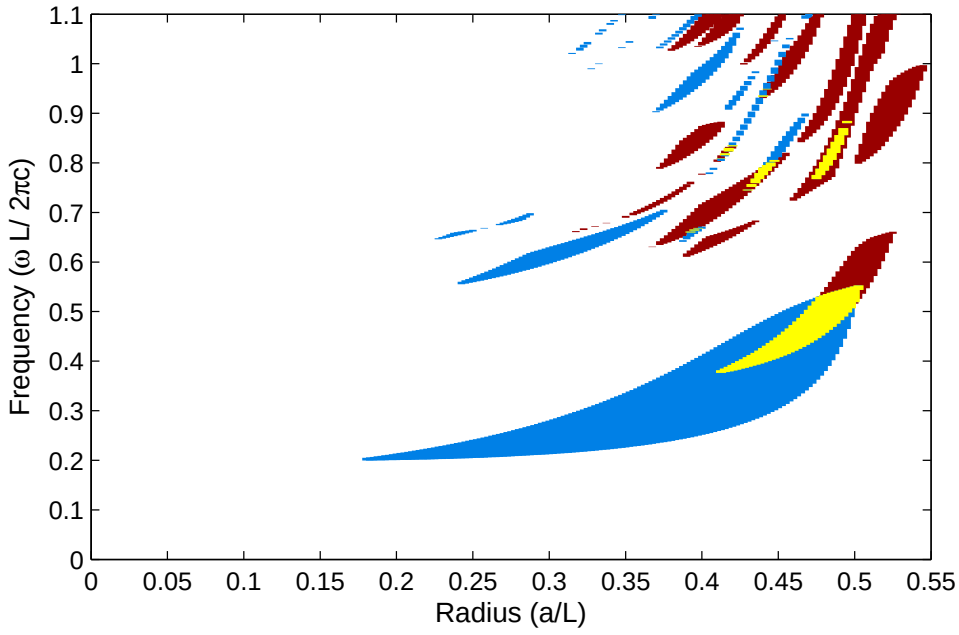

Figure 7: Gap map of a triangular lattice of air columns in a dielectric medium ($\epsilon_2 = 11.4$). The red, blue and yellow regions correspond to bandgaps of E (only), H (only) and both polarizations, respectively.

respectively. The yellow regions represent complete bandgaps for both polarizations. We also calculate the gap map for a triangular lattice of dielectric cylinders in vacuum. The dielectric constant of the cylinders is $\epsilon_1 = 11.4$. Our results are shown in Fig. 8, where the red, blue and yellow regions represent bandgaps for E only, H only and both polarizations, respectively.

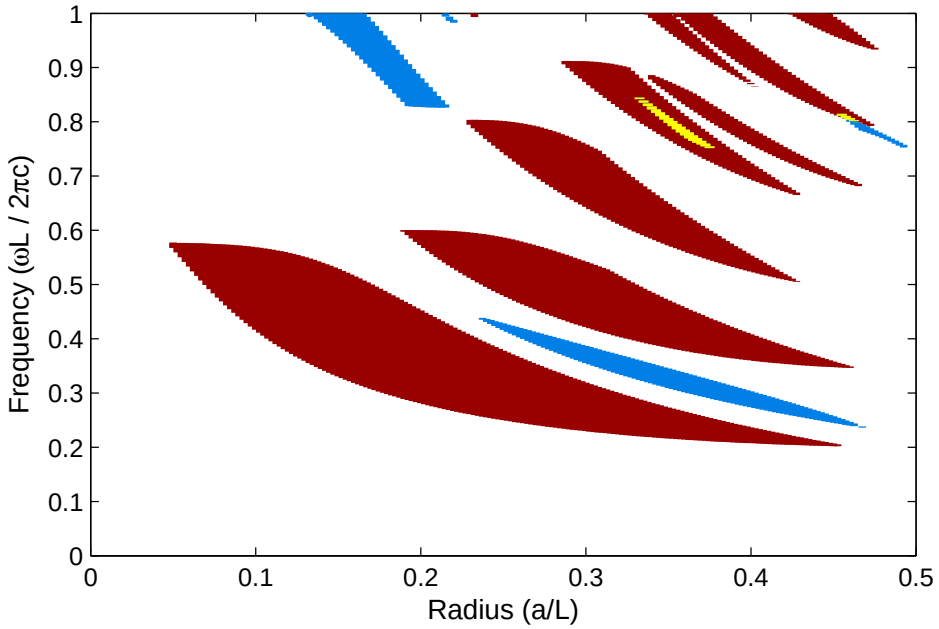

Figure 8: Gap map of a triangular lattice of dielectric cylinders ($\epsilon_1 = 11.4$) in vacuum. The red, blue and yellow regions correspond to bandgaps of E (only), H (only) and both polarizations, respectively.

5 Conclusions

In this paper, we developed an efficient method for computing band structures of two-dimensional photonic crystals composed of triangular lattices of circular cylinders. The method relies on the Dirichlet-to-Neumann map of the hexagon unit cell which is calculated from a cylindrical wave expansion of $6N$ terms, if N collocation points are used on each edge of the hexagon. Unlike existing methods based on cylindrical wave expansions, our method does not need sophisticated lattice sums techniques. An eigenvalue problem for $(12N) \times (12N)$ matrices is formulated for a given frequency, where the eigenvalue is related to the Bloch wave vector. This is a linear eigenvalue problem even if the material is dispersive. Comparing with existing methods, our method is highly competitive, since a small N, say $N \leq 10$, is sufficient for most problems. Our method is particularly suitable for computing the bandgaps directly, that is, without computing the detailed dispersion curves first.

Acknowledgments

This research was partially supported by a grant from the Research Grants Council of Hong Kong Special Administrative Region, China (Project No. CityU 101804).

References

[1] J. D. Joannopoulos, R. D. Meade and J. N. Winn, *Photonic Crystals. molding the flow of light*, Princeton Univ. Press, Princeton, NJ, 1995.

[2] K. M. Leung and Y. F. Liu, "Full vector wave calculation of photonic band structures in face-centered-cubic dielectric media", Phys. Rev. Lett. **65,** 2646–2649 (1990).

[3] Z. Zhang and S. Satpathy, "Electromagnetic wave propagation in periodic structures – Bloch wave solution of Maxwell's equations", Phys. Rev. Lett. **65,** 2650–2653 (1990).

[4] K. M. Ho, C. T. Chan and C. M. Soukoulis, "Existence of a photonic gap in periodic dielectric structures", Phys. Rev. Lett. **65,** 3152–3155 (1990).

[5] R. D. Meade, A. M. Rappe, K. D. Brommer, et al, "Accurate theoretical analysis of photonic band-gap materials", Phys. Rev. B **48,** 8434–8437 (1993).

[6] S. G. Johnson and J. D. Joannopoulos, "Block-iterative frequency-domain methods for Maxwell's equations in a planewave basis", Opt. Express **8,** 173–190 (2001).

[7] D. C. Dobson, "An efficient method for band structure calculations in 2D photonis crystals", J. Comput. Phys. **149,** 363–379 (1999).

[8] W. Axmann and P. Kuchment, "An efficient finite element method for computing spectra of photonic and acoustic band-gap materials: I. Scalar case", J. Comput. Phys. **150,** 468–481 (1999).

[9] H. Y. D. Yang, "Finite difference analysis of 2-D photonic crystals", IEEE Trans. Microwave Theory Tech. **44,** 2688–2695 (1996).

[10] C. P. Yu and H. C. Chang, "Applications of the finite difference mode solution method to photonic crystal structures", Optical and Quantum Electronics **36,** 145–163 (2004).

[11] S. Guo, F. Wu, S. Albin and R. S. Rogowski, "Photonic band gap analysis using finite-difference frequency-domain method", Opt. Express **12,** 1741–1746 (2004).

[12] M. Marrone, V. F. Rodriguez-Esquerre and H. E. Hernández-Figueroa, "Novel numerical method for the analysis of 2D photonic crystals: the cell method", Opt. Express **10,** 1299–1304 (2002).

[13] S. Jun, Y. S. Cho and S. Im, "Moving least-square method for the band-structure calculation of 2D photonic crystals", Opt. Express **11,** 541–551 (2003).

[14] X. Checoury and J. M. Lourtioz, "Wavelet method for computing band diagrams of 2D photonic crystals", Opt. Commun. **259,** 360–365 (2006).

[15] K. M. Leung and Y. Qiu, "Multiple-scattering calculation of the two-dimensional photonic band structure", Phys. Rev. Lett. **48,** 7767–7771 (1993).

[16] N. A. Nicorovici and R. C. McPhedran, "Photonic band gaps for arrays of perfectly conducting cylinders", Phys. Rev. E **52,** 1135–1145 (1995).

[17] K. Ohtaka, T. Ueta and K. Amemiya, "Calculation of photonic bands using vector cylindrical waves and reflectivity of light for an array of dielectric rods", Phys. Rev. B **57,** 2550–2568 (1998).

[18] J. B. Pendry and A. MacKinnon, "Calculation of photon dispersion relations", Phys. Rev. Lett. **69,** 2772–2775 (1992).

[19] J. B. Pendry, "Calculating photonic band structure", *Journal of Physics: Condensed Matter* **8,** 1085–1108 (1996).

[20] L. C. Botten, N. A. Nicorovici, R. C. McPhedran, et al., "Photonic band structure calculations using scattering matrices", Phys. Rev. E **64,** 046603 (2001).

[21] C. T. Chan, Q. L. Yu and K. M. Ho, "Order-N spectral method for electromagnetic waves", Phys. Rev. B **51,** 16635–16642 (1995).

[22] K. Sakoda, N. Kawai, T. Ito, et al, "Photonic bands of metallic systems. I. Principle of calculation and accuracy", Phys. Rev. B **64,** 045116 (2001).

[23] T. Ito and K. Sakoda, "Photonic bands of metallic systems. II. Features of surface plasmon polaritons", Phys. Rev. B **64,** 045117 (2001).

[24] J. Yuan and Y. Y. Lu, "Photonic Bandgap Calculations Using Dirichlet-to-Neumann Maps", J. Opt. Soc. Am. A Vol. 23, pp. 3217-3222, Dec. 2006.

[25] R. L. Chern, C. C. Chang, C. C. Chang and R. R. Hwang, "Two classes of photonic crystals with simultaneous band gaps", Japanese Journal of Applied Physics, Vol. 43, pp. 3484-3490, 2004.

[26] M. Plhal and A. A. Maradudin, "Photonic band gap structure of two-dimensional systems: The triangular lattice", Phys. Rev. B Vol 44, 8565–8571, 1991.

[27] V. Kuzmiak, A. A. Maradudin and F. Pincemin, "Photonic band structures of two-dimensional systems containing metallic components", Phys. Rev. B , Vol 50, 16835–16844, 1994.

[28] V. Kuzmiak, A. A. Maradudin and F. Pincemin, "Photonic band structures of two-dimensional systems fabricated from rods of a cubic polar crystal", Phys. Rev. B Vol 55, 4298–4311, 1997.